

# Contrasts in hydrology between regions of basal deformation and sliding beneath Rutford Ice Stream, West Antarctica, mapped using radar and seismic data

T. Murray,<sup>1</sup> H. Corr,<sup>2</sup> A. Forieri,<sup>1</sup> and A. M. Smith<sup>2</sup>

Received 23 February 2008; revised 17 April 2008; accepted 13 May 2008; published 26 June 2008.

[1] Spatially coincident radar and seismic data collected two weeks apart on Rutford Ice Stream were analyzed to investigate the mechanical and hydrological characteristics of the ice-bed interface. Seismic data allow the differentiation of bed deformation from basal sliding. In radar data, sliding regions are characterised by highly variable permittivity values. We suggest these regions are characterized by small water bodies, possibly a cavity system. In contrast, deforming regions are characterised by consistent, low permittivity, which suggests intimate ice-sediment contact without a distinct interface. However, in deforming regions we identified three bright radar features  $\sim 50$  m wide, consistent in lateral location over distances of 5–10 km up and downstream, and comprised of water less than  $\sim 0.2$  m deep. We interpret these as part of a water evacuation system, most likely canals. Our results emphasise the great potential of radar and seismic techniques in combination to infer basal conditions beneath ice streams. **Citation:** Murray, T., H. Corr, A. Forieri, and A. M. Smith (2008), Contrasts in hydrology between regions of basal deformation and sliding beneath Rutford Ice Stream, West Antarctica, mapped using radar and seismic data, *Geophys. Res. Lett.*, 35, L12504, doi:10.1029/2008GL033681.

## 1. Introduction

[2] Ice streams are the most dynamic features of the Antarctic Ice Sheet, draining about 90% of its mass accumulation [Bamber *et al.*, 2000], and consequently provide a key control on the ice sheet's overall mass balance. Ice stream flow is modulated by three different processes: ice deformation, basal sliding, and bed deformation, with the last two components dominating. Understanding basal processes beneath ice streams, and how ice stream flow is related to and affected by basal conditions and hydrology, is therefore critical for improving models of ice stream dynamics and ice sheet mass balance.

[3] However, the basal environment of ice streams is poorly understood with only a handful of direct observations. Reliance is therefore placed on geophysical methods, such as seismic and radar surveys, which can provide information about ice stream basal conditions (recent examples include Gades *et al.* [2000] and Catania *et al.* [2003]). Using seismic techniques, Vaughan *et al.* [2003] analyzed

the dynamic state (deforming versus non-deforming) of the beds of four Antarctic ice streams, and in two cases (Rutford Ice Stream and Talutis Inlet) showed both lodged (non-deforming) and dilated (deforming) sediments coexisted. Smith *et al.* [2007] showed regions of the bed of Rutford Ice Stream in fact switched between deforming and non-deforming conditions over a 7-year period.

[4] This paper presents and compares unpublished airborne radar data with previously published spatially coincident seismic data [Smith *et al.*, 2007] from Rutford Ice Stream. The seismic data were collected two weeks prior to the radar data. These data sets are used to infer mechanical and hydrological conditions at the basal interface and the relationship between them. Rutford Ice Stream, West Antarctica, is a fast flowing glacier that drains about 36000 km<sup>2</sup> of the West Antarctic Ice Sheet into Ronne Ice Shelf (Figure 1). The ice stream is  $\sim 200$  km long, 20–25 km wide, 2–3 km thick, and the ice flow rate at a location close to the line R2 is around 380 m a<sup>-1</sup> [Murray *et al.*, 2007]. The ice stream is bounded on its western side by the Ellsworth Mountains and on its eastern side by Fletcher Promontory, and it occupies an asymmetric trough, which is deeper on the western side.

## 2. Methods

[5] Radar data were collected during the 2004–2005 field season in the area around 78.1°S, 84.0°W,  $\sim 50$  km upstream of the grounding line (Figure 1). The main data analysed in this paper (R2 on Figure 1) were coincident with a seismic line. The seismic data and its processing methodology are described by Smith *et al.* [2007] and Smith [1997], respectively.

[6] The airborne radar system operated with a transmit power of 4 kW and centre frequency of 150 MHz using bistatic antenna arrays, each of 11 dB gain. A 4  $\mu$ s, 10 MHz chirp pulse was used. Pulse repetition frequency was 15625 Hz and coherent integrations of 50 signals were recorded every  $\sim 40$  cm along track. Sampling frequency was 22 MHz. The aircraft was equipped with a GPS receiver to provide position and a GPS was run on the ice stream to act as a base station. Terrain clearance during the flights averaged  $\sim 260$  m.

[7] The raw radar data were first chirp compressed [Ulaby *et al.*, 1982] but no migration was undertaken. To calculate ice thickness, data were filtered using a 20-trace running mean to reduce trace-trace incoherent noise, and the range delay of the basal echo was identified and picked. Despite large variation in basal reflectivity, the base of the ice stream was identified in every radar trace. We used the calibrated aircraft radar-altimeter data as the surface refer-

<sup>1</sup>School of the Environment and Society, Swansea University, Swansea, UK.

<sup>2</sup>British Antarctic Survey, Natural Environment Research Council, Cambridge, UK.

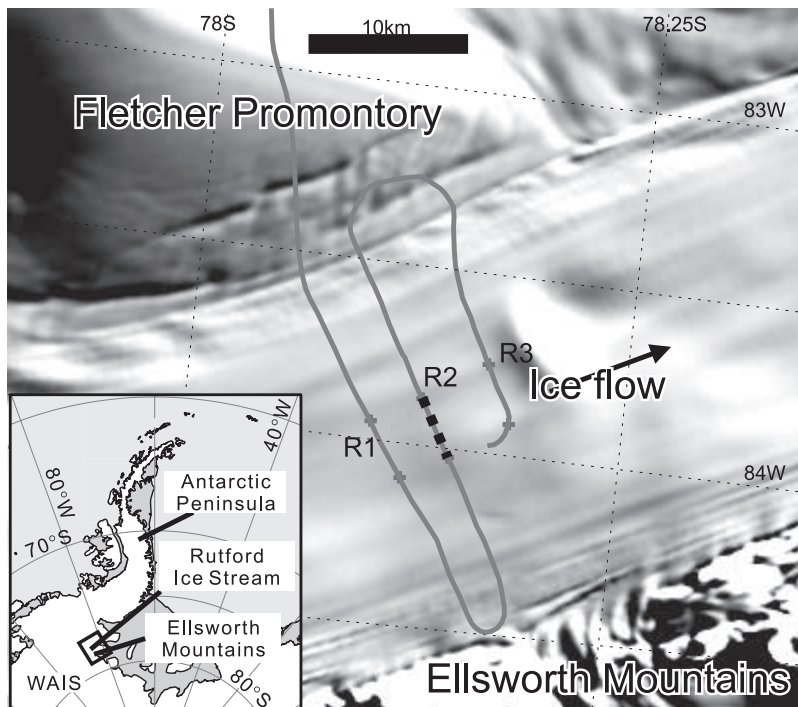


**Figure 1.** Location map showing Rutford Ice Stream and area surveyed during 2004–5 field season. Image background MODIS mosaic of Antarctica [Haran *et al.*, 2005]. Grey line, RES flight; dashed line, R2 coincident radar and seismic data presented in this paper; data from line segment R1 are presented in Figure 3a. WAIS, West Antarctic Ice Sheet.

ence. Electromagnetic wave propagation velocity in the ice was taken to be  $168 \text{ m } \mu\text{s}^{-1}$  [Bogodorosky *et al.*, 1985], and a correction of +10 m was applied to account for the firn layer. The resulting accuracy in ice thickness is estimated to be around  $\pm 20 \text{ m}$  [Vaughan *et al.*, 2006].

[8] The power of the received basal-echo from the radar is dependent on the attenuation characteristics of the ice column and the physical nature of the ice-bed interface. Using the unfiltered data, we calculated the bed reflection power (BRP), defined as one half of the sum of squared amplitude in a particular time window, divided by the number of samples in that window [Gades *et al.*, 2000]. Provided the ice column is homogeneous and the temperature profile does not vary laterally, the energy lost by scattering and absorption within the ice should not change significantly across the area, because the variation in ice thickness is only  $\sim 120 \text{ m}$ . This assumption was confirmed by calculating the internal reflection power (IRP), i.e., the energy per unit sample reflected from the entire ice column. The IRP was nearly constant, showing that variations in the BRP are primarily due to characteristics of the bed and not to changes in the structure of the overlying ice.

[9] To assess basal conditions quantitatively, we calculated the relative dielectric permittivity of the bed by comparing the received power amplitude with that from a portion of the radar flight line over the floating part of Carlson Inlet, where physical properties at the basal interface can be assumed to be seawater with known electrical characteristics (relative dielectric permittivity of 88 and conductivity  $4 \text{ S m}^{-1}$ , giving a power reflection coefficient of  $-1 \text{ dB}$ ). Radar echoes from the ice-water interface of Carlson Inlet are very clear and constant in amplitude,

indicating a smooth and regular reflecting interface. Carlson Inlet is significantly different in thickness ( $\sim 750 \text{ metres}$ ) from Rutford Ice Stream, so it was necessary to correct received power amplitudes to allow a comparison between the two areas. We corrected for geometrical spreading and absorption using a constant value of  $2 \text{ dB} / 100 \text{ m}$  from a site  $\sim 80 \text{ km}$  away with essentially the same surface temperature, accumulation rate and impurity content and hence absorption [Corr *et al.*, 1993]. Uncertainty in the absorption, estimated to be less than  $0.5 \text{ dB} / 100 \text{ m}$ , is thought to be the largest source of error in the calculated permittivities. Assuming that the ratio of the amplitudes from Rutford Ice Stream and Carlson Inlet is the same as the ratio of the reflection coefficient magnitude, it is possible to calculate the reflection coefficient [e.g., Bentley *et al.*, 1998; Peters *et al.*, 2005] beneath Rutford Ice Stream, and using an assumption of planar reflectors it is thus possible to calculate the relative dielectric permittivity of the basal material.

### 3. Results

[10] Figure 2 shows the bed reflector as well as the ice thickness from both the radar and seismic surveys. In the central part of the ice stream, a large bump, about  $400 \text{ m}$  wide and  $50 \text{ m}$  high, is evident (Figures 2d and 2e). The two thickness measurements agree within the accuracy of the techniques (Figure 2e), however, the radar ice thickness profile is rougher due to the larger quantity of data. The maximum difference in ice thickness between the two techniques is  $25 \text{ metres}$  and occurs at  $\text{km } 2.5$  where the reflection amplitudes for both seismic and radar are rela-

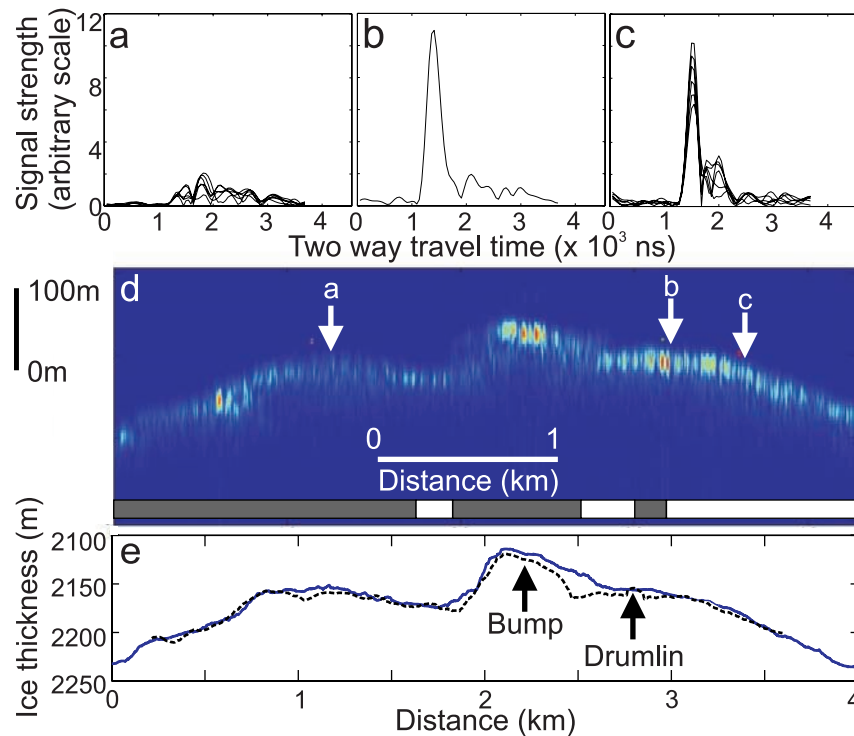


**Figure 2.** Figures 2a–2c show the waveform of reflected radar signal over different bed types. Locations are shown in Figure 2d. (a) Typical region of bed deformation. Note low amplitude and long pulse duration. (b) High reflection strength region, interpreted as fresh water in this paper. Note rapid rise and short pulse duration. (c) Typical region of basal sliding. Note high amplitudes and variability of trace amplitude. Six adjacent traces are shown in Figures 2a and 2c. (d) Radargram showing basal interface of line segment R2; processing consists of horizontal averaging over 20 traces. Figures 2a–2c refer to locations of the waveforms shown. Grey bars depict regions interpreted as deforming and white bars regions of sliding from seismic acoustic impedance. (e) Ice thickness from radar line R2 (solid) and coincident seismic data (dashed). Arrows show location of drumlin and bump referred to in text. In Figures 2d and 2e, ice flow direction is into the page.

tively weak; the range difference falls just within the combined measurement error of the two methods.

[11] While the radar and seismic data give similar ice thicknesses overall, the radar data do not resolve an important subglacial feature identified by *Smith et al.* [2007] using the seismic data. This feature is a subglacial drumlin, ~20 m high and ~100 m wide, comprised of apparently mobile sediment (Figure 2e). Because there is not any fundamental difference in the resolution of the two techniques, it is possible that the feature is obscured by the bright reflector located immediately alongside the drumlin (Figure 2d): the picking algorithm will identify this higher amplitude return in preference to any low amplitude arrival direct from the drumlin itself.

[12] The BRP shows three peaks of strong reflection, at km 0.55, km 2.2 and km 2.9, corresponding to a flat area, the bump, and a location close to the drumlin (Figures 2d and 2e). The reflected wavelet in all of these areas is strong, and shows a rapid rise and short pulse length (Figure 2b). The calculated permittivity values show the same pattern of variability across the ice stream with three major peaks where the relative permittivity is 60–80 (Figure 3b). Away from these peaks, the permittivity can be broadly split into two different categories (Figure 3b) – low values and less variability (km 0–2.5), where the waveform is uniformly prolonged and of low amplitude (e.g., Figure 2a), and

higher values with high variability (between km 2.5 and km 4), where the waveform is intermediate and variable (e.g., Figure 2c). We interpret these variations as resulting from different characteristics at the base of the ice.

#### 4. Discussion and Conclusions

[13] Calculations of bed acoustic impedance from seismic surveys can be compared with the results from the radar data (Figure 3). Acoustic impedance allows discrimination of areas where the flow of ice stream is due to basal sliding or to a deforming bed [*Smith, 1997*], an interpretation supported by passive acoustic emissions [*Smith, 2006*]. The three bright BRP peaks which produce high permittivity peaks are associated with areas of deforming bed (Figures 2d and 2e). Furthermore, in two cases, they appear to correlate with mounds of deforming sediment. Apart from these three regions, the regions we noted as having high and variable permittivity broadly correlate with areas where the ice stream is sliding, and the regions of lower and less variable permittivity with areas of basal deformation (Figure 3b).

[14] Corrected variations in received radar power, and hence permittivity, indicate heterogeneity at the ice-bed interface. In the main sliding regions (km 2.5–2.8 and km 3–4), the magnitude of permittivity peaks are too high

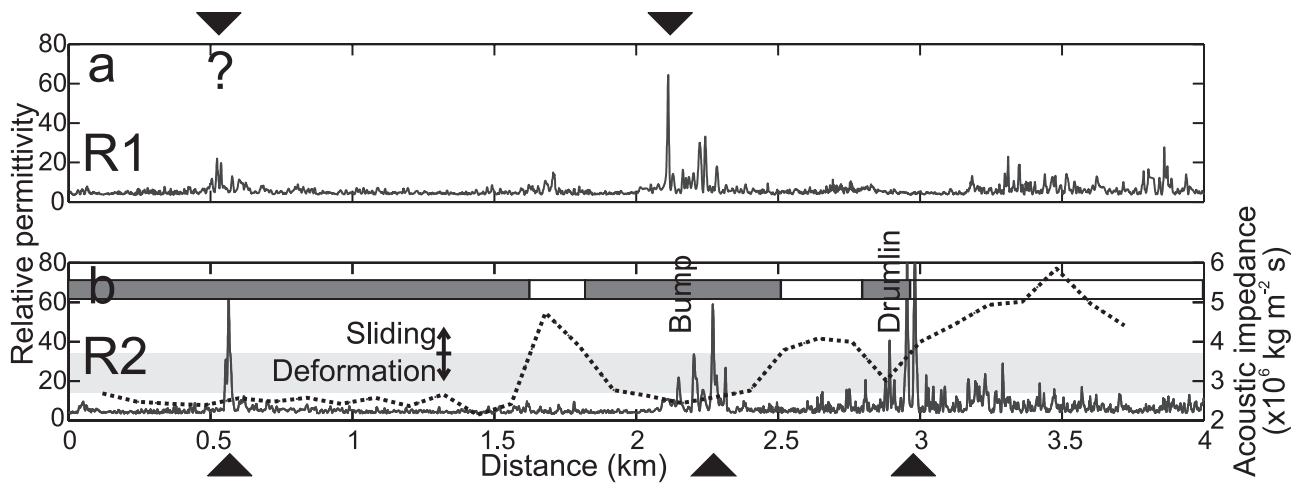


**Figure 3.** Basal relative dielectric permittivity calculated assuming planar interfaces from radar survey as described in text. (a) Segment R1 and (b) segment R2 (solid line) with acoustic impedance (dashed line) from spatially coincident seismic survey conducted two weeks prior to radar collection. Acoustic impedance is sampled every 120 m; the radar is sampled every 0.4 m. Dark grey bars depict regions interpreted as deforming from seismic acoustic impedance and white bars depict regions of sliding. The Bump and Drumlin are labelled at their centres. Light shaded bar on graph shows the approximate range associated with dilated, deforming sediments, including porosities in the range  $\sim 0.35$ – $0.45$  [Smith, 1997]. Triangles indicate high permittivity values. Ice flow direction is into the page.

(Figure 3b) to simply result from a reflection at an ice-sediment interface (the relative permittivity of a porosity 0.3 till is  $\sim 18$ ), and so water must occur in those locations at the bed. This interpretation is supported by the form of the high amplitude echo waveforms in these areas, which are strong and sharp, and characterized by a rapid rise and short tail (e.g., Figure 2c). However, the variability in both the permittivity and waveforms suggests this water must be spatially variable and in relatively small bodies. One possible arrangement of this water would be in cavities at the bed. The contrasting low reflection strength and permittivity in the deforming regions (km 0–1.6, 1.8–2.5 and 2.8–3 in Figures 2a and 3b) suggests that there is no free water at the interface between ice and sediment, and that this interface is rough or indistinct, because otherwise a brighter reflection would be expected.

[15] Because of the very high value of permittivity calculated in the three bright regions (Figures 2d and 3b), the only possible basal interface is a smooth ice-water horizon. Since the site is  $\sim 40$  km upstream of the grounding line, the water is most likely fresh with conductivity  $\sim 5 \times 10^{-4} \text{ S m}^{-1}$ . At 150 MHz, a pure ice-water interface gives a reflection coefficient of  $-3.3$  dB. Our interpretation of a planar ice-water interface is supported by the echo waveforms, which are strong and sharp, and characterized by a regular rapid rise and short tail (e.g., Figure 2b). Thus the permittivity values suggest that fresh water exists in three narrow zones along the radar section in regions of bed deformation. We now consider the likely geometry of these water bodies.

[16] 1. To estimate their width, we note that the minimum radar cross section,  $A$ , required before a return is considered as a planar ice-water interface can be derived from the relationship  $R^2 = 4A^2/\lambda^2$  [Ulaby *et al.*, 1982], where  $R$  is the range and  $\lambda$  is the radar wavelength. At our sites,  $R$  is  $\sim 2500$  m which means a square of side 50 m of water

would meet the minimum criterion. A planar reflector of this size has a focused radiating pattern with a half-power beamwidth of  $< 1^\circ$ , which explains the discrete nature of the returns in the radargram (Figure 2d). Therefore we estimate that the features are  $\sim 50$  m in width.

[17] 2. The distinct high-permittivity peaks are not matched by corresponding changes in the seismic data (Figure 3b), and no second reflector occurs from the base of the water layer in the radar data. These observations show the water bodies must be less than  $\sim 0.2$  m in thickness [King *et al.*, 2004]. An estimate of their minimum thickness is  $\sim \lambda/30$  (below which they would not be resolved [Sheriff, 1991]) and the features must therefore be more than  $\sim 0.04$  m in thickness.

[18] 3. Comparison between this line and parallel radar data collected further upstream and downstream (Figures 1 and 3a) suggests that some of these features are continuous along  $\sim 5$ – $10$  km of bed. However, our radar line separation is greater than two ice thicknesses, and the geometry of such a hydrological network on a rough bed will be under-sampled: ponds of water fortuitously aligned along flow on each line would produce similar radargrams.

[19] We suggest that these bright, high permittivity regions are water that forms part of a channelised or canalized hydrological system (cf. observations by Engelhardt and Kamb [1997]). Because they occur in regions of deforming bed and the surface slope is low, theory would suggest they are most likely to be canals [Walder and Fowler, 1994; Ng, 2000]. This is supported by the lack of a change in the ice thickness above the features, which suggests they are eroded down into basal sediments rather than up into the ice. The features are considerably wider than the 3–5 m predicted by theory [Ng, 2000], or inferred ( $\sim 1$  m) by Engelhardt and Kamb [1997] from borehole hydraulic experiments. However, the features are narrower than a canal interpreted from seismic data by King *et al.* [2004].



[20] From these observations we can make three important inferences about the nature of the hydrological system and basal interface beneath the ice stream.

[21] 1. We have observed discrete, possibly linear water bodies that appear to be associated with regions of deforming bed, and in two cases with long basal topographic features (the bump and drumlin), which are composed of deforming sediments. We argue these permittivity highs most likely result from wide, low canals at the ice stream interface, and form part of a water evacuation system. We note that the existence of canals requires continual erosion of basal sediments to remove the influx of deforming sediment, but this cannot explain the erosion observed by *Smith et al.* [2007], because that occurred on regions of glacier sliding rather than deformation.

[22] 2. Sliding appears to be associated with considerable spatial variability in the permittivity, and distinctly contrasts with the generally low permittivity in deforming regions. We infer that the ice-bed interface in sliding regions is much wetter than in regions where the bed is undergoing deformation. Because the permittivity peaks are too high simply to result from water-saturated till, water must occur at the bed. We suggest there are numerous small water bodies or cavities at the ice-bed interface where the ice stream is sliding over its bed and none where the ice is deforming its bed. The cavities may be the product of fast sliding, or may be necessary for facilitating sliding by reducing the interface friction.

[23] 3. The primarily weak and indistinct reflection in regions of bed deformation suggests intimate contact between ice and bed, but without a distinct ice-sediment interface. This presumably reflects the need for coupling between ice and bed for deformation to occur.

[24] It is clear that the two methods, seismic and radar uniquely complement one other for basal process studies. Seismic interpretations reveal the bulk properties of the material beneath the ice base, whereas radar reflectivity measurements are governed by the interface between the ice and its substrate, and reveal basal hydrology. However, by effectively calibrating the radar with temporally-coincident seismic data, we have shown the potential to map regions of sliding and deformation in radar data because of spatially-coincident changes in basal hydrology. Since radar data are much faster to collect than seismic data, this raises the exciting possibilities of producing a virtual snapshot of basal processes over much larger areas of ice-stream bed than has been previously possible. The characterization of the ice-stream bed for a single epoch has the potential to add considerably to studies of glacial landforms and processes, particularly when coupled with models of ice dynamics.

[25] **Acknowledgments.** Funding was provided by NERC/AFI (GR3/G005) and British Antarctic Survey (BAS). Field support was provided by

BAS. TM was supported by a Leverhulme Trust Fellowship. We thank Captain David Leatherdale for help with radar data acquisition.

## References

- Bamber, J. L., D. G. Vaughan, and I. Joughin (2000), Widespread complex flow in interior of Antarctic Ice Sheet, *Science*, *287*, 1248–1250.
- Bentley, C. R., N. Lord, and C. Liu (1998), Radar reflections reveal a wet bed beneath stagnant Ice Stream C and a frozen bed beneath ridge BC, West Antarctica, *J. Glaciol.*, *44*, 149–156.
- Bogodorosky, V. V., C. R. Bentley, and P. E. Gudmandsen (1985), *Radio-glaciology*, Reidel, Dordt, Netherlands.
- Catania, G. A., H. B. Conway, A. M. Gades, C. F. Raymond, and H. Engelhardt (2003), Bed reflectivity beneath inactive ice streams in West Antarctica, *Ann. Glaciol.*, *36*, 287–291.
- Corr, H., J. C. Moore, and K. W. Nicholls (1993), Radar absorption due to impurities in Antarctic Ice, *Geophys. Res. Lett.*, *20*, 1071–1074.
- Engelhardt, H., and B. Kamb (1997), Basal hydraulic system of a West Antarctic ice stream: Constraints from borehole observations, *J. Glaciol.*, *43*, 207–230.
- Gades, T. M., C. F. Raymond, H. Conway, and R. W. Jacobel (2000), Bed properties of Siple Dome and adjacent ice streams, West Antarctica, inferred from radio echo-sounding measurements, *J. Glaciol.*, *46*, 88–94.
- Haran, T., J. Bohlander, T. Scambos, and M. Fahnestock (Eds.) (2005), MODIS mosaic of Antarctica (MOA) image map, <http://insidc.org/data/moa/>, Natl. Snow and Ice Data Cent., Boulder, Colo.
- King, E. C., J. Woodward, and A. M. Smith (2004), Seismic evidence for a water-filled canal in deforming till beneath Rutford Ice Stream, West Antarctica, *Geophys. Res. Lett.*, *31*, L20401, doi:10.1029/2004GL020379.
- Murray, T., M. A. King, A. M. Smith, and G. Weedon (2007), Ice flow modulated by tides at up to annual periods at Rutford Ice Stream, West Antarctica, *Geophys. Res. Lett.*, *34*, L18503, doi:10.1029/2007GL031207.
- Ng, F. S. L. (2000), Canals under sediment-based ice sheets, *Ann. Glaciol.*, *30*, 146–152.
- Peters, M. E., D. D. Blankenship, and D. L. Morse (2005), Analysis techniques for coherent airborne radar sounding: Applications to West Antarctic ice streams, *J. Geophys. Res.*, *110*, B06303, doi:10.1029/2004JB003222.
- Sheriff, R. E. (1991), *Encyclopedic Dictionary of Exploration Geophysics*, 3rd ed., Soc. of Explor. Geophys., Tulsa, Okla.
- Smith, A. M. (1997), Basal condition on Rutford Ice Stream, West Antarctica, from seismic observations, *J. Geophys. Res.*, *102*, 543–552.
- Smith, A. M. (2006), Microearthquakes and subglacial conditions, *Geophys. Res. Lett.*, *33*, L24501, doi:10.1029/2006GL028207.
- Smith, A. M., T. Murray, K. W. Nicholls, K. Makinson, G. Aðalgeirsdóttir, A. Behar, and D. G. Vaughan (2007), Rapid erosion and drumlin formation observed beneath a fast-flowing Antarctic ice stream, *Geology*, *35*, 127–130.
- Ulaby, F. T., R. K. Moore, and A. K. Fung (1982), *Microwave Remote Sensing: Active and Passive*, vol. II, *Radar Remote Sensing and Surface Scattering and Emission Theory*, Addison-Wesley, Reading, Mass.
- Vaughan, D. G., A. M. Smith, P. C. Nath, and E. Le Meur (2003), Acoustic impedance and basal shear stress beneath four Antarctic ice streams, *Ann. Glaciol.*, *36*, 225–232.
- Vaughan, D. G., H. F. J. Corr, F. Ferraccioli, N. Frearson, A. O'Hare, D. Mach, J. W. Holt, D. D. Blankenship, D. D. Morse, and D. A. Young (2006), New boundary conditions for the West Antarctic ice sheet: Subglacial topography beneath Pine Island Glacier, *Geophys. Res. Lett.*, *33*, L09501, doi:10.1029/2005GL025588.
- Walder, J. S., and A. Fowler (1994), Channelized subglacial drainage over a deformable bed, *J. Glaciol.*, *40*, 3–15.

H. Corr and A. M. Smith, British Antarctic Survey, Natural Environment Research Council, Madingley Road, Cambridge CB3 0ET, UK.

A. Forieri and T. Murray, School of the Environment and Society, Swansea University, Singleton Park, Swansea SA2 8PP, UK. (t.murray@swansea.ac.uk)